Bull. Mater. Sci., Vol. 32, No. 3, June 2009, pp. 337–342. © Indian Academy of Sciences.

Synthesis, structure and photocatalytic properties of β-$ZrMo_2O_8$

PRANGYA PARIMITA SAHOO, S SUMITHRA, GIRIDHAR MADRAS and T N GURU ROW*

Solid State and Structural Chemistry Unit, Indian Institute of Science, Bangalore 560 012, India

Abstract. **Monoclinic $ZrMo_2O_8$ was synthesized via solid state method and single crystals of the title compound have been grown by the hydrothermal method. The crystals belong to monoclinic crystal system with space group $C2/c$ (No. 15) with $a = 11{\cdot}4243(19)$ Å, $b = 7{\cdot}9297(6)$ Å, $c = 7{\cdot}4610(14)$ Å and $\beta = 122{\cdot}15(2)°$, $Z = 4$. The bandgap of the compound was 2·57 eV. Unlike the other polymorphs of $ZrMo_2O_8$, the monoclinic form has unique crystallographic features with ZrO_8 and Mo_2O_8 polyhedra. The photocatalytic activity of this compound has been investigated for the first time for the degradation of various dyes under UV irradiation and has been compared with the photoactivity of the trigonal form of $ZrMo_2O_8$. It has been observed that this compound exhibits specificity towards the degradation of cationic dyes.**

Keywords. **Zirconium molybdate; crystal growth; X-ray diffraction; crystal structure; photocatalysis; dye degradation.**

1. Introduction

$ZrMo_2O_8$ is one of the well studied compounds in recent literature particularly with reference to its polymorphic modifications, phase transitions and negative thermal expansion. The structural flexibility associated with this molecule allows itself to be adopted to various polymorphic forms. Amongst them, at ambient pressure the most stable polymorphs are the α and β forms. The single crystal structure of α-$ZrMo_2O_8$ was solved in trigonal crystal system with space group $P\bar{3}1c$ (No. 163) with $a = 10{\cdot}1391(6)$ Å, $c = 11{\cdot}7084(8)$ Å and $Z = 6$ (Auray *et al* 1986). They have also solved the structure of the β-$ZrMo_2O_8$ in the monoclinic crystal system with space group $C2/c$ (No. 15) with $a = 11{\cdot}4309(3)$ Å, $b = 7{\cdot}9376(2)$ Å, $c = 7{\cdot}4619$ (2) Å and $\beta = 122{\cdot}323$ (2)°, $Z = 4$ (Auray *et al* 1989). In the same year, Klevtsova *et al* (1989) reported the single crystal structure of this polymorph and published the coordinates of all the constituent atoms. It is also to be noted that the negative thermal expansion materials, viz. the cubic and the orthorhombic LT-$ZrMo_2O_8$ have also been prepared via careful dehydration of the precursor, $ZrMo_2O_7(OH)_2{\cdot}2H_2O$ at 365–390°C and 300°C, respectively (Lind *et al* 1998; Allen *et al* 2003). The linear thermal expansion coefficients are $-5{\cdot}0 \times 10^{-6}$ K^{-1} and $-1{\cdot}2 \times 10^{-6}$ K^{-1} for the cubic and the LT polymorphs, respectively.

Under the influence of temperature and pressure the polymorphs of $ZrMo_2O_8$ undergo phase transitions. The monoclinic to trigonal transformation occurs at around 690°C (Auray *et al* 1989). The cubic form undergoes a phase transformation to the trigonal form above 390°C and this behaviour has been studied via time resolved X-ray diffraction (Lind *et al* 2002). Further, the trigonal form (α-$ZrMo_2O_8$) undergoes a second order phase transition at around 215°C to α'-$ZrMo_2O_8$ with space group $P\bar{3}m1$ (No. 164) with $a = 5{\cdot}8460(6)$ Å, $c = 5{\cdot}9941(8)$ Å (Allen *et al* 2004). Two completely reversible phase transitions occur for α-$ZrMo_2O_8$ at 1·06–1·11 GPa and 2·0–2·5 GPa, respectively. The phases have been named as δ and ε phases and they belong to the monoclinic and triclinic crystal systems, respectively (Carlson and Andersen 2000; Andersen and Carlson 2001). High pressure studies using Raman, infrared, optical absorption spectra and resistance measurements on trigonal polymorph have been performed recently and show the consistency of the spectroscopic techniques with the diffraction results (Muthu *et al* 2002; Karandikar *et al* 2006). High pressure X-ray diffraction experiments on cubic $ZrMo_2O_8$ have revealed a first order phase transition above 0·7 GPa when compressed hydrostatically and under non-hydrostatic condition amorphization commences above 0·3 GPa (Lind *et al* 2001). The simultaneous application of both temperature and pressure on the cubic form generates the stable α-trigonal and the β-monoclinic forms (Grzechnik and Crichton 2002).

Apart from negative thermal expansion, various other properties have been analyzed. For example, $ZrMo_2O_8$ gel finds important applications as inorganic ion exchangers (Clearfield and Blessing 1972; Monroy-Guzmán *et al* 2003). The trigonal $ZrMo_2O_8$ consists of ZrO_6 octahedra and MoO_4 tetrahedra wherein the fourth oxygen atom O(4) points towards the interlayer region. This feature gives rise to various properties like resistance, luminescence and more recently catalysis (Blasse and Dirksen

*Author for correspondence (ssctng@sscu.iisc.ernet.in)

1987; Karandikar *et al* 2006; Sahoo *et al* 2009). In order to develop novel energy storage devices, lithium and sodium insertion to monoclinic and trigonal form has been attempted. The monoclinic structure could accept up to two Li atoms per formula unit whereas amorphization occurred for the trigonal polymorph (Sudorgin *et al* 2009).

Semiconductor photocatalysis is an area of interest in environmental remediation ever since the discovery of the most widely used photocatalyst, TiO_2 (Fujishima and Honda 1972). In recent years focus is on non-TiO_2 based catalysts which have resulted in evaluation of photocatalytic properties of $PbBi_2Nb_2O_9$, $BiVO_4$ and $ZnWO_4$ (Kudo *et al* 1999; Kim *et al* 2004; Fu *et al* 2006).

In our recent work, we have discussed the photocatalytic activity of the trigonal form of $ZrMo_2O_8$ synthesized via two different routes, viz. the routine solid state technique and the combustion synthesis method (Sahoo *et al* 2009). To the best of our knowledge, there has been no report of the catalytic activity of various polymorphs of $ZrMo_2O_8$. The previous reports on the single crystal structure determination of the monoclinic $ZrMo_2O_8$ did not treat the atoms anisotropically. Further, the current datasets have been obtained on a four circle diffractometer with a very high precision and the determination of the structure is rigorous. In the current paper, we discuss the synthesis, single crystal growth, crystal structure and photocatalytic activity of the thermodynamically stable monoclinic polymorph and compare its activity with the trigonal form.

2. Experimental

2.1 *Materials*

ZrO_2 was synthesized by heating $Zr(NO_3)_4{\cdot}5H_2O$ (BDH England, 99%) for 4 h at 550°C. MoO_3, methylene blue (MB), orange G (OG), rhodamine B (RB), remazol brilliant blue R (RBBR), malachite green (MG) and congo red (CR) (all from S.D. Fine-Chem Ltd., India) were used. Water was double distilled and filtered through a Millipore membrane filter prior to use.

2.2 *Synthesis and crystal growth*

For the preparation of monoclinic β-$ZrMo_2O_8$, ZrO_2 and MoO_3 were taken in the ratio of 1 : 2. The heat treatment was conducted according to the procedure mentioned in the literature (Auray *et al* 1989). The composition was ground well and the resulting mixture was fired at 600°C for 48 h with a heating rate of 10°C/min with an intermediate grinding after 24 h.

The crystals were grown by hydrothermal method. The monoclinic $ZrMo_2O_8$, synthesized by solid state method was taken as the starting material for obtaining the single crystals. Approximately 0·5 g of the monoclinic sample was transferred to a Teflon lined autoclave. Then 15 mL of distilled water was added, stirred for 15 min and then kept in an oven at 180°C for 5 days. The resultant product was filtered out and dried in air. Very small colourless crystals appeared on the surface of the product. Crystals suitable for X-ray diffraction were carefully selected under the microscope.

2.3 *Characterization*

2.3a *Single crystal X-ray diffraction*: A colourless plate like single crystal was selected on the basis of size and sharpness of diffraction spots. Data collection was carried out on an Oxford Xcalibur MOVA diffractometer using a graphite monochromatized MoKα wavelength ($\lambda_{MoK\alpha}$ = 0·71073 Å) radiation at 293(2) K. The data were reduced using special programs available with the diffractometer. The structure was solved by direct methods using SHELXS97 and refined using SHELXL97 (Sheldrick 1997). Crystallographic data and the details of the single-crystal data collection are given in table 1. Atomic coordinates and isotropic displacement parameters are presented in table 2. Anisotropic displacement parameters (ADPs) and selected inter atomic distances are given in tables 3 and 4. The bond valence sums were calculated (Brown and Shannon 1973; Brown and Altermatt 1985) and are given in table 4.

Table 1. Crystallographic data collection and structure refinement of monoclinic $ZrMo_2O_8$.

Empirical formula	$ZrMo_2O_8$
Formula weight	411·10
Crystal habit, colour	Plate, colourless
Crystal size (mm)	0·017 × 0·010 × 0·007
Temperature (K)	293(2)
Radiation	Molybdenum
Wavelength (Å)	0·71073
Crystal system	Monoclinic
Space group	*C*2/*c*
a (Å)	11·4243(19)
b (Å)	7·9297(6)
c (Å)	7·4610(14)
β (°)	122·15(2)
Volume (Å^3)	572·3(2)
Z	4
Density (g cm^{-3})	4·771
F(000)	752
Scan mode	ω scans
θ_{max} (°)	32·7
$h_{min,max}$, $k_{min,max}$, $l_{min,max}$	(–17, 17), (–11, 11), (–11, 11)
No. of reflns measured	992
No. of unique reflns	902
μ (mm^{-1})	4·576
No. of parameters	52
Refinement	F^2
*R*_all, *R*_obs	0·0219, 0·0187
wR_2_all, wR_2_obs	0·0425, 0·0419
GoF	1·073
Max, min $\Delta\rho$ (e/Å^3)	0·876, –0·845

Table 2. Atomic coordinates (Å) and isotropic displacement parameters (Å^2) for monoclinic $ZrMo_2O_8$.

Atomic and Wyckoff position	*x*	*y*	*z*	U_{eq} (Å^2)	Occupancy
Zr(4*e*)	0	–0·01766(4)	0·25	0·0045(1)	1
Mo(8*f*)	0·21495(2)	0·27919(3)	0·25770(3)	0·0071(1)	1
O(1)(8*f*)	0·0926(2)	0·1147(2)	0·0769(3)	0·0085(5)	1
O(2)(8*f*)	0·3464(2)	0·3368(2)	0·5617(3)	0·0109(5)	1
O(3)(8*f*)	0·3511(2)	0·2984(3)	0·2119(3)	0·0110(5)	1
O(4)(8*f*)	0·1290(2)	0·4615(3)	0·1678(4)	0·0201(6)	1

Table 3. Anisotropic displacement parameters (Å^2) of monoclinic $ZrMo_2O_8$.

Atom	U_{11}	U_{22}	U_{33}	U_{23}	U_{13}	U_{12}
Zr	0·0041(2)	0·0050(1)	0·0040(2)	0	0·0018(1)	0
Mo	0·0073(1)	0·0083(1)	0·0052(1)	–0·0012(1)	0·0030(1)	–0·0029(1)
O(1)	0·0077(8)	0·0100(8)	0·0077(9)	–0·0017(7)	0·0041(7)	–0·0020(6)
O(2)	0·0114(8)	0·0155(9)	0·0061(9)	–0·0034(7)	0·0048(7)	–0·0072(7)
O(3)	0·0106(9)	0·0152(9)	0·0078(9)	–0·0026(7)	0·0053(8)	–0·0047(7)
O(4)	0·0173(10)	0·0139(10)	0·0199(11)	–0·0027(8)	0·0038(9)	0·0016(8)

Table 4. Selected bond lengths of monoclinic $ZrMo_2O_8$.

Bond length type	Distance (Å)	Bond length type	Distance (Å)
Mo–O(1)	1·862(2)	Zr–O(1) × 2	2·312(2)
Mo–O(2)	1·995(2)	Zr–O(1)′ × 2	2·217(2)
Mo–O(2)′	2·039(2)	Zr–O(2) × 2	2·118(2)
Mo–O(3)	1·768(3)	Zr–O(3) × 2	2·142(3)
Mo–O(4)	1·674(2)		
BVS	5·962	BVS	4·202

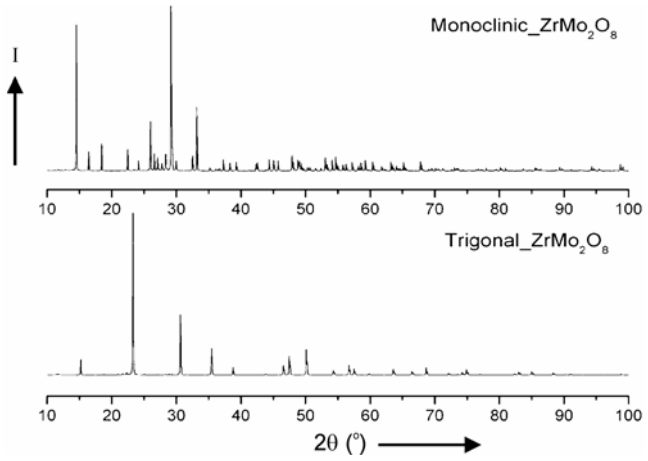

Figure 1. Powder X-ray diffraction patterns of monoclinic and trigonal $ZrMo_2O_8$.

2.3b *Powder X-ray diffraction and UV-vis spectra*: Powder X-ray diffraction data were collected using the Philips X-pert Pro diffractometer with CuKα radiation over the angular range $10° \leq 2\theta \leq 100°$, with a step width of 0·02°. Powder diffraction data show the formation of a single phase compound for monoclinic $ZrMo_2O_8$. For comparison, the powder diffraction patterns of the monoclinic and the trigonal forms are given in figure 1.

Le Bail profile analysis in the *JANA2000* suite was used to refine the X-ray diffraction data (Dušek *et al* 2001). The background was estimated by Legendre polynomial, and the peak shapes were described by a pseudo-Voigt function varying five profile coefficients. The experimental, calculated and the difference profiles for monoclinic $ZrMo_2O_8$ are presented in figure 2.

The UV-vis diffuse reflectance spectra were recorded on a Perkin Elmer Lambda 35 UV-vis Spectrophotometer. The bandgap calculated for the monoclinic form is 2·57 eV as compared to 2·74 eV for the trigonal polymorph (Sahoo *et al* 2009). Figure 3 shows the solid state UV diffuse reflectance spectra of the monoclinic and the trigonal polymorphs.

2.4 *Photocatalytic experiments*

2.4a *Photochemical reactor*: The photochemical reactor used in this study has two parts. The inner part is a jacketed quartz tube whereas the outer part is a pyrex glass reactor. A high pressure mercury vapour lamp (HPML) of 125 W (Philips, India) was placed after the

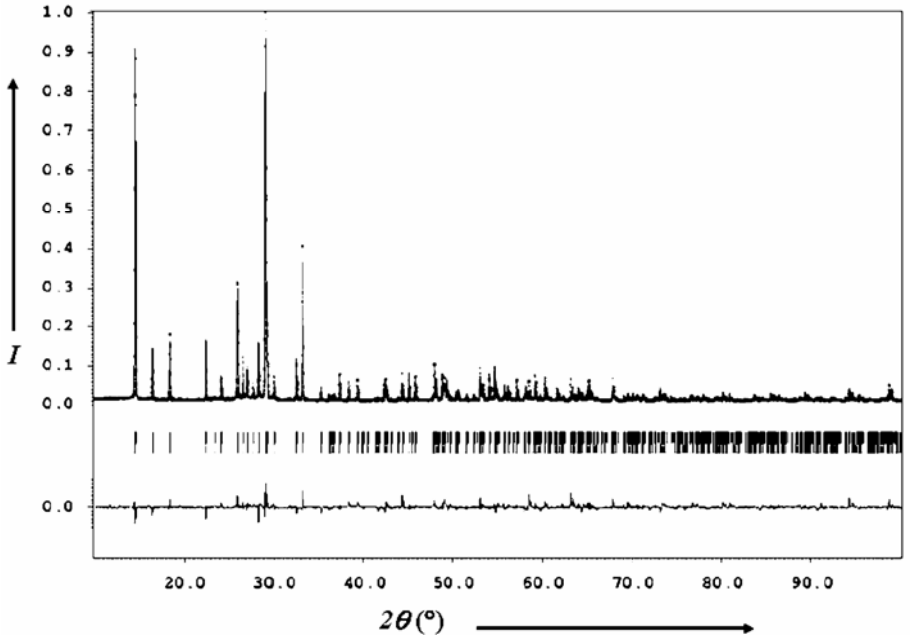

Figure 2. Experimental (dashed) and calculated (solid line) X-ray diffraction profiles of monoclinic $ZrMo_2O_8$. The difference profile is located at the bottom.

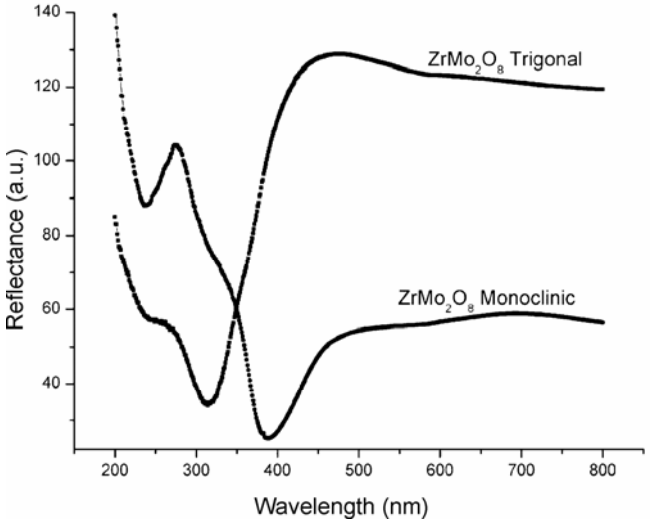

Figure 3. Diffuse reflectance spectra of monoclinic and trigonal $ZrMo_2O_8$.

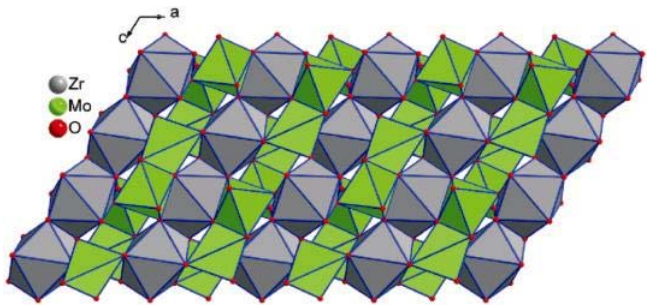

Figure 4. Structure of monoclinic $ZrMo_2O_8$ along *b* axis.

removal of the outer shell. Water circulates through the annulus of the quartz tube, maintaining the temperature of the suspension at ambient temperature. 100 ml of the solution is taken into the outer reactor and continuously stirred to ensure that the suspension of the catalyst is uniform. The lamp radiated primarily at 365 nm. Extensive details of the experimental set up are provided elsewhere (Sivalingam *et al* 2003).

2.4b *Degradation experiments*: The initial concentrations in the dye solutions varied between 15 and 100 ppm depending on the molar absorptivity (ε) of each dye. The catalyst loading was 0·1 g and the volume of the dye solution taken was 100 mL in all the experiments. The solution was stirred for 1 h in dark to account for any adsorption. 4 mL of the solution was drawn 6 times over a span of 1 h for UV experiments. The samples were filtered through Millipore membrane filters and centrifuged to remove the catalyst particles prior to UV analysis.

2.4c *Sample analysis*: All samples were analysed with a UV-visible spectrophotometer (Lambda 35, Perkin-Elmer) to quantify the degradation reactions. The calibration for MB, OG, RB, RBBR, CR and MG were based on Beer–Lambert law at their maximum absorption wavelengths, λ_{max} of 664, 489, 554, 591, 497 and 615 nm, respectively. The analysis of the samples using UV-vis spectrophotometer showed a continuous decrease in the UV-vis absorption at λ_{max} of the dye.

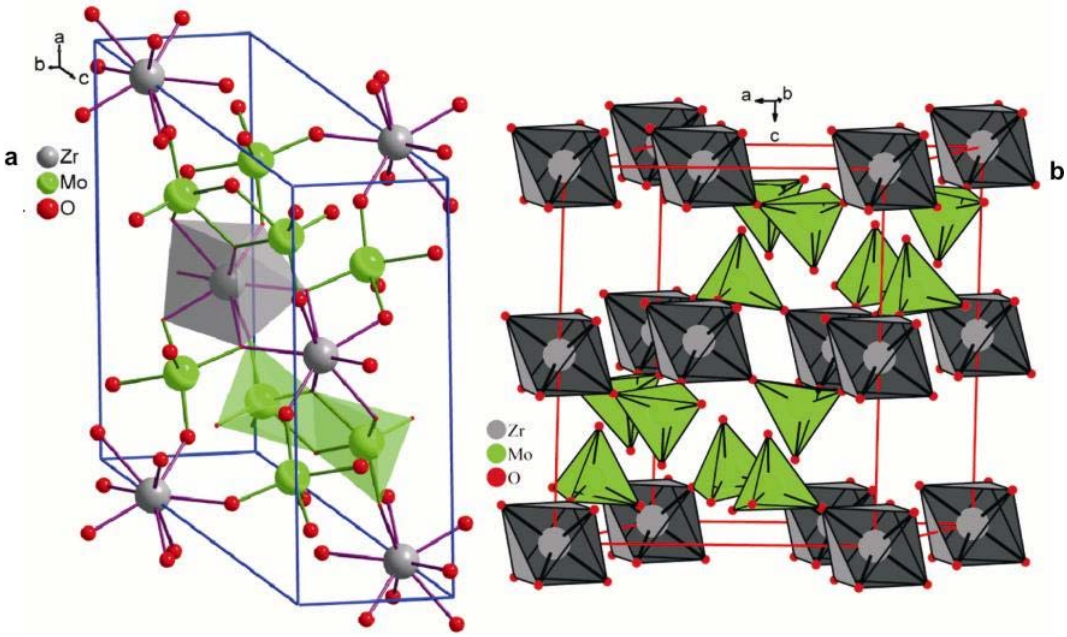

Figure 5. Polyhedral arrangement in the unit cell of **a**. monoclinic and **b**. trigonal $ZrMo_2O_8$.

3. Results and discussion

3.1 *Crystal structure*

The structure was solved from 902 unique reflections having $I \geq 2\sigma$. The positions of Zr and Mo were determined using direct methods. The difference Fourier synthesis allowed locating the oxygen atoms. The structure has one zirconium, one molybdenum and four oxygen atoms. Zirconium occupies the special position (two fold symmetry, Wycoff 4*e*), whereas molybdenum and oxygen atoms occupy general positions (8*f*). Full occupancies were assigned to all the atoms. The final residual factors are $R_1 = 0{\cdot}0187$ and $wR_2 = 0{\cdot}0419$.

Zirconium is eight coordinated. ZrO_8 polyhedra share edges forming a three dimensional network. Molybdenum is five coordinated and forms a tetragonal pyramidal structure. Two MoO_5 polyhedra share edges with each other forming Mo_2O_8 moieties. It is noteworthy that the structure has MoO_5 polyhedra unlike the other polymorphs where molybdenum forms MoO_4 tetrahedra. Further, monoclinic polymorph depicts a unique ZrO_8 polyhedral coordination whereas the other polymorphs of $ZrMo_2O_8$ have ZrO_6 octahedra. These features are quite distinct from the other polymorphs of $ZrMo_2O_8$. The arrangement of the polyhedra along *b* axis in the structure is presented in figure 4. The comparison between the monoclinic and the trigonal forms in terms of the polyhedral arrangement in the crystal structure is shown in figure 5.

The Mo–O bond lengths vary from 1·674(2) to 2·039(2) Å. The Zr–O bond lengths vary from 2·118(2) to 2·312(2) Å. Molybdenum is coordinated with all four kinds of oxygen atoms whereas zirconium is coordinated with O(2), O(3) and O(1) oxygen atoms. Bond valence sums were calculated for molybdenum and zirconium atoms. For molybdenum atom, the value is 5·962 whereas for zirconium atom the value is 4·202.

3.2 *Photocatalysis*

Photocatalytic degradation of the dyes MB, OG, RB, RBBR, CR and MG was investigated. The lamp position in the photochemical reactor was adjusted such that no degradation occurred in the absence of UV light or the catalyst alone. Figure 6 shows the profiles of dye degradation in presence of monoclinic $ZrMo_2O_8$. It was observed that anionic dyes like OG and RBBR do not degrade in presence of this catalyst.

Among the cationic dyes that degraded, the following order was evident with the initial rates of degradation being 0·233, 0·400, 0·100 and 0·183 (ppm/min) for MB, CR, RB and MG, respectively. If a first order is assumed, the rate coefficients are 0·0031, 0·0051, 0·0111 and 0·0131 min^{-1}, respectively. The catalytic behaviour of the monoclinic polymorph is different from that of the trigonal polymorph. In our previous studies (Sahoo *et al* 2009), we have shown that the trigonal $ZrMo_2O_8$ could degrade all the dyes that do not contain the anthraquinonic group. However, this polymorph could not degrade any anionic dyes. Further studies are required to determine the reason of this specificity.

4. Conclusions

Monoclinic $ZrMo_2O_8$ was synthesized by solid state technique and the single crystals were grown hydrothermally.

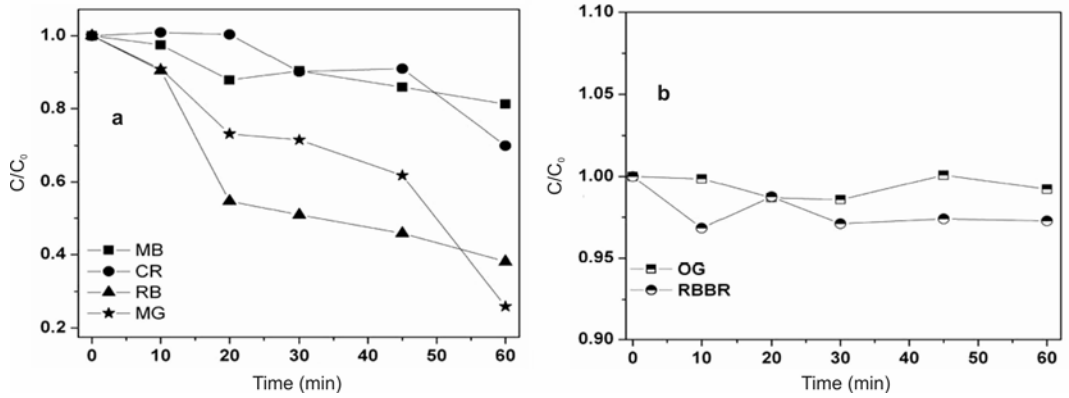

Figure 6. UV degradation of various **a**. cationic dyes and **b**. anionic dyes in presence of monoclinic $ZrMo_2O_8$.

The photocatalytic activity of this polymorph has been studied for the first time. Since the reports available on the crystal structure of monoclinic modification of $ZrMo_2O_8$ were not rigorously accurate, we report the single crystal structure of the title compound. This reveals the difference in crystallographic features between the monoclinic and the trigonal modifications. The structure of monoclinic $ZrMo_2O_8$ consists of ZrO_8 and Mo_2O_8 polyhedra unlike the other polymorphs of $ZrMo_2O_8$ including the trigonal form. The trigonal modification was found to be specific towards the degradation of non-anthraquinonic dyes whereas the monoclinic modification was found to be specific towards the degradation of cationic dyes. Hence, we emphasize the role of crystal structure in inducing the photocatalytic activity and specificity towards different class of dyes. The photocatalytic activity differs mainly due to the difference in bandgap originating from the crystallographic differences.

Supporting information available

CIF: the crystal data have been deposited at the Fachinformationszentrum Karlsruhe (FIZ) with the number CSD 420668.

Acknowledgements

One of the authors (PPS) thanks the Indian Institute of Science for a senior research fellowship. We acknowledge funding from DRDO and DST, India. We thank DST-FIST, India for funding the single crystal X-ray CCD facility.

References

Allen S, Warmingham N R, Gover R K B and Evans J S O 2003 *Chem. Mater.* **15** 3406
Allen S, Ward R J, Hampson M R, Gover R K B and Evans J S O 2004 *Acta Crystallogr.* **B60** 32
Andersen A M K and Carlson S 2001 *Acta Crystallogr.* **B57** 20
Auray M, Quarton M and Tarte P 1986 *Acta Crystallogr.* **C42** 257
Auray M, Quarton M and Tarte P 1989 *Powder Diffraction* **1** 29
Blasse G and Dirksen G J 1987 *J. Phys. Chem. Solids* **48** 591
Brown I D and Shannon R D 1973 *Acta Crystallogr.* **A29** 266
Brown I D and Altermatt D 1985 *Acta Crystallogr.* **B41** 244
Carlson S and Andersen A M K 2000 *Phys. Rev.* **B61** 11209
Clearfield A and Blessing R H 1972 *J. Inorg. Nucl. Chem.* **34** 2643
Dušek M, Petříček V, Wunschel M, Dinnebier R E and van Smaalen S 2001 *J. Appl. Crystallogr.* **34** 398
Fu H, Lin J, Zhang L and Zhu Y 2006 *Appl. Catal.* **A306** 58
Fujishima A and Honda K 1972 *Nature* **238** 37
Fujishima A, Rao T N and Tryk D A 2000 *J. Photochem. Photobiol. C*: *Photochemistry Reviews* **1** 1 (and the references therein)
Grzechnik A and Crichton W A 2002 *Solid State Sci.* **4** 1137
Karandikar A S, Mukherjee G D, Vijayakumar V, Godwal B K, Achary S N and Tyagi A K 2006 *J. Appl. Phys.* **100** 013517
Kim H G, Hwang D W and Lee J S 2004 *J. Am. Chem. Soc.* **126** 8912
Klevtsova R F, Glinskaya L A, Zolotova E S and Klevtsov P V 1989 *Dokl. Akad. Nauk SSSR* **305** 91
Kudo A, Omori K and Kato H 1999 *J. Am. Chem. Soc.* **121** 11459
Lind C, Wilkinson A P, Hu Z, Short S and Jorgensen J D 1998 *Chem. Mater.* **10** 2335
Lind C, VanDerveer D G, Wilkinson A P, Chen J, Vaughan M T and Weidner D J 2001 *Chem. Mater.* **13** 487
Lind C, Wilkinson A P, Rawn C J and Payzant E A 2002 *J. Mater. Chem.* **12** 990
Monroy-Guzmán F, Díaz-Archundia L V and Ramírez A C 2003 *Appl. Radiat. Isot.* **59** 27
Muthu D V S, Chen B, Wrobel J M, Andersen A M K, Carlson S and Kruger M B 2002 *Phys. Rev.* **B65** 064101
Sivalingam G, Nagaveni K, Hegde M S and Madras G 2003 *Appl. Catal.* **B45** 23
Sahoo P P, Sumithra S, Madras G and Guru Row T N 2009 *J. Phys. Chem.* **C113** 10661
Sheldrick G M 1997 *SHELXL97 Program for crystal structure refinement* (Germany: University of Gottingen)
Sudorgin N G, Nalbandyan V B and Shukaev I L 2008 *Solid State Ionics* **179** 503